Preprints of the 21st IFAC World Congress (Virtual)
Berlin, Germany, July 12-17, 2020

Optimal Hierarchical Control of DC Microgrids: modelling and experimental validation

Marcel Pendieu Kwaye, Riccardo Maria Vignali, Riccardo Lazzari

RSE S.p.A., Milan, Italy
(Tel: +390239924780; e-mail: {marcel.pendieukwaye, riccardo.vignali, riccardo.lazzari}@rse-web.it).

Abstract: DC Microgrids are receiving a growing interest thanks to the advantages offered by the integration of renewable sources. This paper presents an optimal hierarchical control for DC microgrids that performs multiple control objectives, like (i) voltage regulation, (ii) minimization of the losses, (iii) power-sharing, (iv) energy storage management and (v) economic savings. The hierarchical control is made up of sequential actions so that, at the higher level, the optimal plan for power generators and for storage systems is generated and then sent to the model predictive control. This controller is the core of this study and it has three main functions such as (i) voltage regulation, (ii) energy storage management and (iii) tracking of the optimal planning, taking into account the different characteristics of the DC components and generating the references for the low-level controller. The proposed control based on optimization has been validated with good results on the real low-voltage DC microgrid in RSE.

Keywords: DC Microgrid, Hierarchical control, Optimal power flow, Model predictive control, Optimization problems.

1. INTRODUCTION

In the last years, economic, technological and environmental aspects are leading to a considerable revision of the traditional power system. To achieve the primary goal of decarbonisation, the main trends are focused on the incorporation of renewable energy sources (RESs), on the spread adoption of electric vehicle (EVs) and on the improvement in energy efficiency at all level. In this context, the integration of DC microgrids (MGs) in the traditional power system can provide different advantages like higher efficiency (Pellegrino & Lazzari, 2018) and the natural interface with RESs, electronic loads, EVs and energy storage systems (ESSs) (Dragicevic, et al., 2014). For all these reasons, DC microgrids are attracting growing interest and are receiving much research attention.

DC microgrids are active and independent distribution systems that can manage and control all the resources in order to reduce the exchange of power with the main power system, to achieve economic savings and to ensure a proper operation in all the system conditions (Meng, et al., 2017). The MGs management and control are multi-objective tasks, which cover different time scale and physical level: *i)* local voltage and current control to satisfy stability requirements; *ii)* voltage regulation to ensure the proper operation of the connected generators and loads; *iii)* current or power sharing to prevent the overstressing of the sources; *iv)* management of power and energy to balance energy sources and reduce power flow losses; *v)* scheduling of the resources, to achieve economic savings and to reduce the power exchange with the main power system.

However, control schemes are usually designed to just achieve voltage regulation and current or power sharing. Droop control is a common method to fulfil, by means of parallel converters without communication, the regulation of a common DC bus voltage. There are several shortcomings, that limit the performance of droop control, such as load-dependent voltage deviation and current sharing deterioration caused by not negligible lines' impedances (Dragičević, et al., 2016). The development of hierarchical controllers are thus necessary to achieve the current sharing. This goal can be achieved resorting to different heuristic solutions (Papadimitriou, et al., 2015) or dealing with optimization problem on power management taking into account the different characteristics of each component (Iovine, et al., 2019). Hierarchical control has also been used for economic operation, resilience enhancement (Liang & Mohammad, 2014) and to ensure proportional load sharing and improvements of voltage regulation in distribution DC microgrids (Sandeep, et al., 2013).

Nevertheless, the current sharing requirement does not permit the regulation of the voltage at each node towards its corresponding nominal value (Cucuzzella, et al., 2018). A reasonable alternative goal is to control the average voltage across the whole microgrid to a global voltage level (Nasirian, et al., 2015). In any case, the solution does not take into account the voltage deviation at the not-controllable nodes, where are connected the loads and the RESs. A direct voltage control and power-sharing can be achieved resorting to optimal power flow (OPF) techniques that allows, through the control of power flow, the minimization of losses and the voltage regulation at each node of the DC microgrid.

In this work, a hierarchical control capable of reaching multiple objectives in a subsequent scheduling manner is proposed. The core of this hierarchical control is based on model predictive control (MPC) with three different goals: (i) voltage regulation, (ii) energy storage management and (iii) tracking the day-ahead scheduled profile (Eghtedarpour & Farjah, 2012). Relaying on the quadratic constraints equations of the network and the low-level controller, the dynamic behaviour of the MPC is discretized in fixed time step while the quadratic constraints are defined in a fixed time horizon. In the MPC formulation, the classical approach, based on energy management flow, is extended, including the power flow equations, in order to take into account the low-level control of the converters on a finite time horizon. In this way, the proposed control fulfils different control goals acting on the cost function of the optimization problems.

Furthermore, our hierarchical scheme involves a high-level controller that deals with an optimization problem considering the economical aspect. It is based on energy management system (EMS) which computes when to purchase and when to sell energy to the grid at a convenient price possibly exploiting arbitrage.

The paper is organized as follows: Section 2 presents in detail the hierarchical control formulations and the links between each controller; Section 3 briefly presents the RSE's microgrid and lastly details the proposed case under study; Section 4 presents the results obtained after the performed test while some conclusions are drawn in Section 5.

2. HIERARCHICAL CONTROL STRUCTURE

The hierarchical control is made in a sequential way with a higher level that is responsible to generate the optimal plan for the controllable components of the system and to ensure economic savings for the next day. In this work, the system under analysis, is constituted by a DC MG, connected to the main power system and composed by PV, loads and energy storage systems. Furthermore, the DC microgrid allows the operation of a small portion of a secondary AC grid composed by a PV and a Load. A schematic representation of the considered framework is depicted in Fig. 1, while the block diagram of the hierarchical control scheme is depicted in Fig. 2.

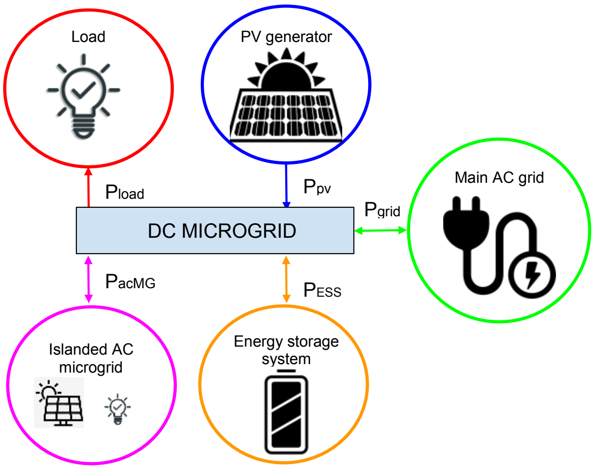

Fig. 1. Representation of the considered framework

In the considered framework, the controllable variables for the higher control level are the power exchanged with the main AC grid and the power exchanged with the energy storage systems. Indeed, acting on the power exchanged, by the ESSs and the DC microgrid, it is possible to regulate the exchanged power with the main AC grid and to reduce the energy cost. The EMS outputs act as an input to the model predictive controller. The latter generates the reference signals for the low-level controllers of the static generators in the network. The model predictive approach (L.Darby, et al., 2009) allows to achieve, at the same time, the voltage regulation, losses minimisation and tracking of the references originated from EMS.

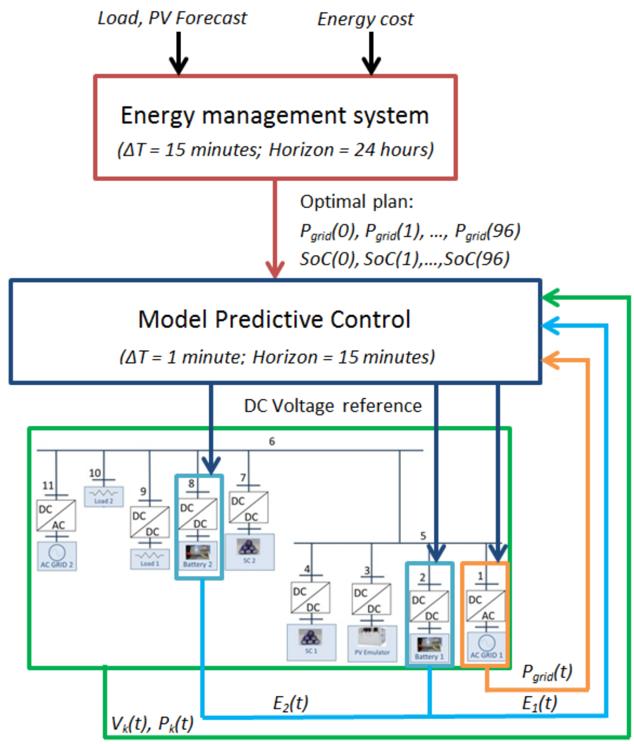

Fig. 2. Block diagram of the hierarchical control scheme

2.1 Energy Management System

The energy management system generates the optimal profile in an economic point of view. The objective of this planning phase is to optimize battery's energy and power during the day in order to satisfy the load demand with the given PV production. This has been done taking into account generation and load forecasts, and the costs of purchasing/selling energy. For this reason, the cost function considered in the optimization problem is composed of the cost of purchasing energy from the network and the revenue obtained from the sale of electricity produced in excess, as expressed in (1).

$$J_3 = \sum_{i=1}^{n} [c_p(i) P_{grid}(\mathrm{i}) - c_s(i)\big(P_{tot}(i) - P_{load}(i)\big)]\Delta T \qquad (1)$$

where c_p, P_{grid}, c_s, P_{tot}, P_{load} are respectively the cost of the purchased energy, the grid power, the selling energy price, the total power generated (from PV power and storage) and the load power. Finally, ΔT is the sampling period, settled equal to 15 minutes; the overall period of 24 hour is thus divided in 96 time steps.

During the optimization process, the physical constraints related to the maximum allowable power and to the battery state of charge must be taken into account, as expressed in (2). In addition to these described operating constraints, it is possible to insert constraints on the status of the components at the end of the day, such as the request that the state of charge of the battery is equal to the state of charge at the beginning of the day.

$$\begin{gathered}\min_{P_{ESS}(i)} \; J_3 \\ 0 \le P_{grid}(i) \le P_{grid}^{max} \\ 0 \le P_{tot}(i) - P_{load}(i) \le P_{grid}^{max} \\ P_{ESS}^{min} \le P_{ESS}(i) \le P_{ESS}^{max} \\ E_{ESS}(i+1) = E_{ESS}(i) - \frac{P_{ESS}^{dch}(i)}{\eta_{dch}}\Delta T + P_{ESS}^{ch}(i)\eta_{ch}\Delta T \\ P_{tot}(i) = P_{PV}(i) + P_{ESS}(i) \\ P_{ESS}(i) = P_{ESS}^{ch}(i) - P_{ESS}^{dch}(i) \\ E_{ESS}(96) = E_{ESS}(0) = E_{ESS0} \\ i = 1,\dots,96 \end{gathered} \tag{2}$$

In (2), P_{ESS} and E_{ESS} are the battery's power and energy in charged or discharge mode, η_{dch} and $\eta_{ch}$are the battery's efficiency and P_{PV} is the power of the PV generator. P_{ESS}^{min} and P_{ESS}^{max} are the minimum and maximum limit of the battery energy, P_{grid}^{max} represents the maximum power exchanged from the grid, P_{tot} is the total power from PV generators and batteries storage systems, P_{ESS}^{ch} and P_{ESS}^{dch} are the ESS's power in charge and discharge mode.

2.2 Model Predictive Controller

The proposed model predictive control ensures the achievement of a broad category of control objectives (e.g, voltage regulation, energy storages management, tracking the optimal plan scheduled by the EMS), by simply tuning some of the cost function parameters. The strategy relies on the solution of a quadratic constrained quadratic program (QCQP), comprising of both the classical network constraints and the low-level control models of the converters. In the QCQP, the dynamics of the system is discretized with a fixed time step ΔT equal to 60 seconds and the constraints are defined on a fixed time horizon T of 15 minutes. Once the optimization is completed, the first sample of the computed optimal control sequence is applied, the state is measured, and the optimization is carried over again, in a receding horizon fashion. With the fact that the MPC works with a temporal scale of minutes, it is not important to consider the electromagnetics transient in the network model. For this reason, in the following, all the electrical quantities will be supposed constant function of time. The relation between all voltages and current injections (positive if outgoing from the node) at a given time t, is expressed by:

$$I(t) = G \cdot V(t) \tag{3}$$

where $G \in R^{n\times n}$ is the matrix of admittances, $I(t) = [I_1(t),\dots,I_n(t)]'$ is the vector containing the current injections for each node, $V = [V_1(t),\dots,V_n(t)]'$ is the vector containing the voltages of each node and n indicates the number of nodes of the network.

From (3), using the definition of electrical power, it is possible to compute the power for each node via:

$$P_k(t) = V_k(t)\left(\sum_{i=1}^{n} G_{ki}V_i(t)\right), \qquad k = 1,\dots,N. \tag{4}$$

Equation (4) describes the relation between all the voltages and electrical powers in the network at a given time. In addition, it is considered also the presence of static generators that, equipped with a droop control, act as voltage sources. For them the relation between the power and the voltage is given by:

$$V_k(t) = V_{ref_k}(t) - D_k P_k(t), \quad k \in \mu. \tag{5}$$

In (5), μ represents the set of nodes of the static converters, $D_k \ge 0$ is the droop coefficient and V_{ref_k} is the reference signal that has to be computed by the MPC scheme. In case of static generators working as grid-forming converters, the coefficient D_k in (5) should be set to zero.

A typical goal, in secondary control, is to maintain the voltage in a desired bound, that it does not violate the operative limits of the network. This requirement leads to the introduction of the following constraints on each node:

$$V_k^{min} \le V_k(t) \le V_k^{max}. \tag{6}$$

Where the voltage limits V_k^{min} and V_k^{max} can be specified as well as a function of time. In a similar way, the power provided by the static generator should be maintained in a desired bound:

$$P_k^{min} \le P_k(t) \le P_k^{max}. \tag{7}$$

Furthermore, in the considered framework, some energy storage systems are connected to the network through the controlled static generators. To take into account these components, in the MPC, the batteries are modelled considering the state of energy $E_k(t)$ as first order integrators:

$$E_k(t + \Delta T) = E_k(t) - P_k(t), \quad k \in \mu. \tag{8}$$

Where P_k is the power of the ESS and it is positive during discharge phase. For each storage system, the dynamics can be rewritten in the more compact matrix form:

$$E_k^t = \mathbf{1}E_k(t) + \boldsymbol{A}P_k^t \tag{9}$$

where $\mathbf{1} = [1,1,\dots,1]'$ is a column vector of ones and matrix $\boldsymbol{A}$ is a lower triangular matrix:

$$\boldsymbol{A} = \begin{bmatrix} -\mathbf{1} & \mathbf{0} & \mathbf{0} \\ \vdots & \ddots & \mathbf{0} \\ -\mathbf{1} & \dots & -\mathbf{1} \end{bmatrix}.$$

Incorporating constraints on upper and lower bound on storage energy leads to:

$$\mathbf{1}E_k^{min} \leq \mathbf{1}E_k(\bar{t}) + \boldsymbol{A}P_k^t \leq \mathbf{1}E_k^{max} \quad (10)$$

Where $E_k(\bar{t})$ represents the state of energy at the first instant and E_k^{min},E_k^{max} are respectively the lower and the upper bound of the energy.

Finally, considering the grid equation (4), the low-level controller (5) and the constraints (6), (7), (10), the online deterministic problem addressed by the MPC strategy can be expressed as:

$$\begin{gathered} \min_{\substack{V_k \; k=1,\dots,n, \\ V_{ref_k} \; k\in\mu \\ P_k \; k\in\mu}} J_2(V, P, t) \\ P_k(t) = V_k(t)\left(\sum_{i=1}^{n} G_{ki}V_i(t)\right) \quad k = 1, \dots, N \\ V_k(t) = V_{ref_k}(t) - D_k P_k(t) \quad k \in \mu \\ V_k^{min} \leq V_k(t) \leq V_k^{max} \\ \mathbf{1}E_k^{min} \leq \mathbf{1}E_k(\bar{t}) + \boldsymbol{A}P_k^t \leq \mathbf{1}E_k^{max} \\ t = \bar{t}, \dots, \bar{t} + T \end{gathered} \quad (11)$$

In (11), the optimization variables are the voltage amplitude of each node: $V_k, k = 1, \dots, N$, the reference voltage for static generators: $V_{refk}, k \in \mu$, and the power injections in the static generators nodes: P_k, $k \in \mu$. Note that, in order to solve problem, a measure of the state of energy at the first time instant $E_k(\bar{t}), k \in \mu$, is needed.

The solution of the problem is the optimal sequence of reference voltages V_{refk}^{opt} of the low level controller of the static generators, the corresponding optimal values of powers P_k^{opt} and the optimal voltages of each node V_k^{opt} that minimize the cost function J_2. Note that the introduction of storage systems makes the model dynamical, i.e., introduces a coupling between the electrical quantities in the network at different time steps. All the quantities appearing in (11) both the control variables and the power injections in non-controllable nodes are defined on the time horizon $[\bar{t}, \dots, \bar{t} + T]$. This means that for the non-controllable variables a forecast is needed. Lastly, the cost function J_2 of problem can be tuned so as to satisfy different control objectives. In the cost function (11), it has been inserted the quadratic sum deviation from desired profile weighted with time variant coefficient for voltage, power and storage energy:

$$J_V = \sum_k \sum_t c_{V_k}(t)\big(V_k(t) - V_k^*(t)\big)^2, \quad (12)$$

$$J_P = \sum_{k\in\mu} \sum_t c_{P_k}(t)(P_k(t) - P_k^*(t))^2, \quad (13)$$

$$J_E = \sum_{k\in\mu} \sum_t c_{E_k}(t)(E_k(t) - E_k^*(t))^2. \quad (14)$$

A further term J_{loss} can be introduced in the cost function for losses minimization:

$$J_{loss} = c_{loss} \textstyle\sum_{k\in\mu} \sum_t P_k(t). \quad (15)$$

The complete cost function is given by the sum of terms (12)-(15):

$$J_2 = J_V + J_P + J_E + J_{loss}. \quad (16)$$

The terms c_{V_k}, c_{P_k}, $c_{E_k}$and c_{loss} are the cost coefficient. These parameters can be modified in order to adjust the behaviour of the controller and to achieve different regulation.

2.3 Low-level Controller

The low-level controller is designed to control independently the multiple resources connected to the dc grid. In general, these resources are connected to the dc grid, through static converters, like dc/dc converters for ESSs and PV generators and ac/dc converters for the interface with ac grid.

In general, low-level controller enables a specific goal at a time, on the basis of the specific objectives (Liu, et al., 2017). The dc/dc converters of the PV generators, and in general of the DERs, track maximum power point to achieve the fully use of the local renewable source and they operate as constant power source. In the opposite way, the ac/dc converters at the interface between the ac and the dc grid normally regulate the bus voltage at a constant value. In addition, in the case of multiple ac/dc interfaces some converters can also operate as constant power source to regulate better the power exchanged between the two grids. The dc/dc converters of the ESSs allow the charge or discharge taking into account their SoC, but these converters can also operate with backup functionalities. In this case, the converter regulates the voltage of the dc grid.

Furthermore, in presence of multiple converters, it can regulate the voltage, the droop control is a common method used to fulfil the regulation of the common DC bus voltage (Dragičević, et al., 2016), but other control based on sliding mode (Cucuzzella, et al., 2018) or passivity (Cucuzzella, et al., 2019) can be used without any additional droop regulation.

From the MPC point of view, the converters regulating the power are seen as injection node, while the converters working as voltage regulation are modelled as a slack node, with or without droop regulation, as expressed in (5).

3. SYSTEM UNDER TEST

3.1 Description of the microgrid

The proposed control scheme has been validated resorting to the DC microgrid of RSE (Ronchegalli & Lazzari, 2016). This LVDC network is unipolar with a nominal voltage level of 380 V and presents two ac/dc converters, of about 100 kVA and 30 kVA, that it allows the exchange of power with the AC grid. The network is also equipped with different ESSs as batteries and supercapacitors. The ESSs are two high-temperature NaNiCl batteries, each with a rated power of 32 kW and a capacity of 18 kWh, along with two supercapacitor (SC) banks, each with a rated power of 30 kW for 10 s. Each battery and supercapacitor bank are coupled to the DC grid through a 35 kW dc/dc bidirectional converter. Finally, one programmable purely resistive load-bank with a maximum power of 30 kW, one constant power load of 30 kW and a PV emulator of 30 kW are installed in the DC microgrid. The layout of the grid is reported in Fig. 3.

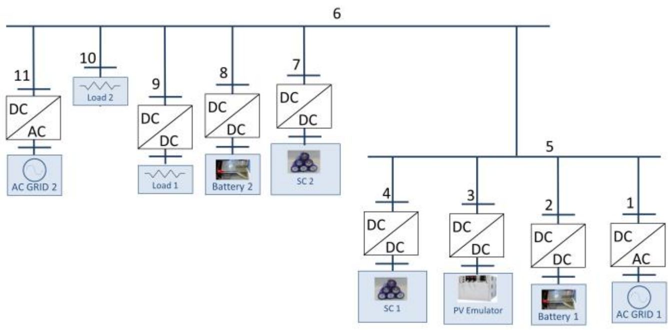

Fig. 3. Layout of the RSE's DC Microgrid

3.2 Hierarchical control implementation

The RSE's DC microgrid allows the experimental verification of different controllers. Indeed, the control of each converter can be implemented in Simulink® and integrated in the dSPACE® controllers of the DC microgrid.

In the considered framework, the converter connected to the AC grid1 provides the voltage regulation of the DC microgrid without any droop control. The battery converters provide the voltage regulation with a droop function as in (5), while the supercapacitor converters are used to compensate very fast fluctuations in the dc voltage as explained in (Grillo, et al., 2014). The load is controlled to exactly follow its reference, while the PV converter is regulated with a maximum power point tracking algorithm. Finally, the ac/dc converter connected to the AC grid2 is working as a grid forming, providing the frequency and the voltage regulation of a secondary islanded AC grid. This secondary islanded grid includes a PV generator and a load.

In the secondary control level, the different behaviour of the converters should be considered. In particular, the load, the PV and the AC grid2 converter are represented as power injection node, while the batteries' converters and the converter connected to the AC grid1 are represented as a voltage node as shown in Fig. 2. Lastly, the supercapacitors' converters are not considered in the secondary control because their dynamics are faster than the fixed time step of 60 seconds used in this control level.

The target of the MPC is to compute the references for the low-level controller while receiving targets for the next 24 hours from the EMS. In the proposed optimal hierarchical control, the MPC receives the desired energy level and power exchanged with the AC grid1 and provides the reference voltage for controllable nodes in order to satisfy (11). The MPC requires the DC grid voltage measurement, the SOC measurements and the electrical power exchanged between the DC microgrid and the main AC grid (Oliveira, et al., 2017).

Furthermore, the MPC requires a proper forecast strategy for the fixed time horizon of 15 minutes. In this work, the future PV, load and AC grid2 power disturbances over the MPC horizon are considered as a constant value. This forecast strategy provides good results with a simpler methodology compared to other forecasting strategy. Considering this forecast strategy, and thanks to its receding horizon implementation, the MPC is still able to achieve feedback and compensation of the last observed disturbances.

3.4 Case study

To verify the behaviour of the proposed optimal hierarchical control applied to the framework illustrated in Fig. 1, a case study with real data, shown in Fig. 4, has been analysed.

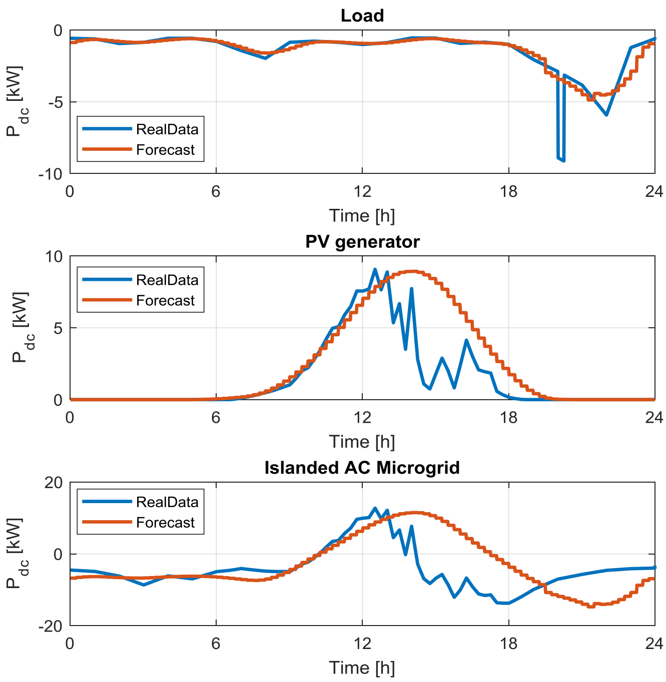

Fig. 4. Forecast and real data used in the test

The selected case study presents the real powers of the injection node, which are similar to the forecast during the first 12 hours and different during the rest of the day. This characteristic allows the verification of the ability of the model predictive controller l to compensate forecast errors.

This concept would be fulfilled only when the forecast economic planning profile from the tertiary control for the exchanged power connection point (PCC) and/or the state of charge of the batteries would be closer to the MPC control output profiles at the secondary level of control. It should be pointed out that, both power tracking and SoC tracking can't be reached in presence of significant forecast errors. However, acting on the cost coefficient of (16) it is possible to pursue different regulation. In the validation of the concept, described in the next section, it is considered to better track the SoC profile. This enables the better usage of the batteries during the days guaranteeing enough energy for the back-up functionality, and to reach the final state of charge, that allows the full usability of the ESSs during the next day.

In the case study, the parameters of the MPC are set as expressed in Table 1. Moreover, the droop coefficient for the batteries' converters are equal to 0.27 V/kW.

Table 1. Nominal, minimum and maximum values of the DC microgrid parameter

Parameter	Nominal	min	max
SOC	45 %	20 %	78 %
Node Voltage	380 V	361 V	399 V
Conv1 Voltage	380 V	372.4 V	387.6 V
Battery Power	0 kW	- 10 kW	10 kW
Conv1 Power	0 kW	- 30 kW	30 kW

4. EXPERIMENTAL RESULTS

Starting from the forecast depicted in Fig. 4, the EMS generates the plan for the main grid active power and for the SOC of the two batteries during the plan horizon of 24 hours, as shown in Fig. 5.

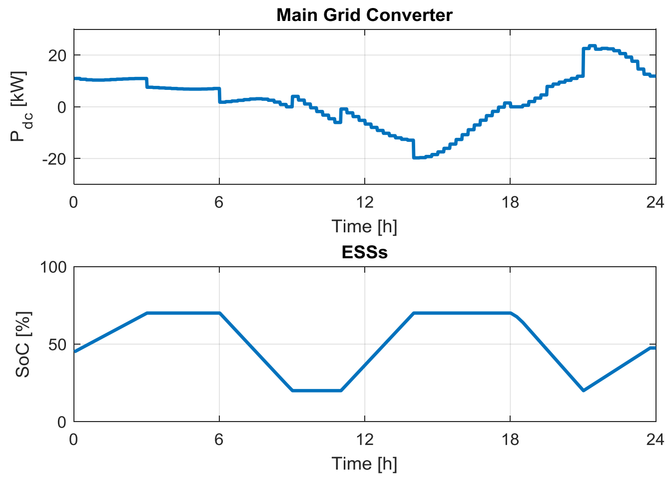

Fig. 5. Energy management system output

Fig. 6 shows the comparison power exchanged between the DC microgrid and the main AC grid during the test. It is worth noting that during the first 12 hours the control tracks the optimal plan, while in the following 12 hours, due to high forecast errors the plan can't be followed. Nevertheless, as shown in Fig. 7 the batteries' SOC tracks its plan without significant errors. In this way, the requirement on the finally state of charge is achieved. Furthermore, the power sharing between the two batteries as well as the energy storage management objective, have been reached.

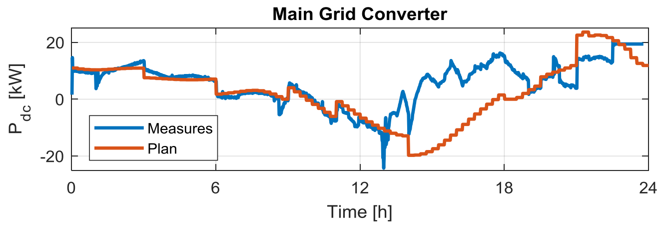

Fig. 6. DC power of the main grid converter

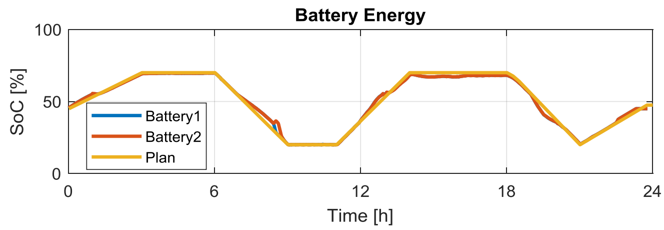

Fig. 7. Batteries state of charge

In Fig. 8 all the node voltages at each time step are shown. Since all the measures are close to each other, the result seems a band. During the entire test, the voltage of the overall DC microgrid is regulated inside the defined boundary, demonstrating again the ability of the proposed controller to achieve different objectives at the same time.

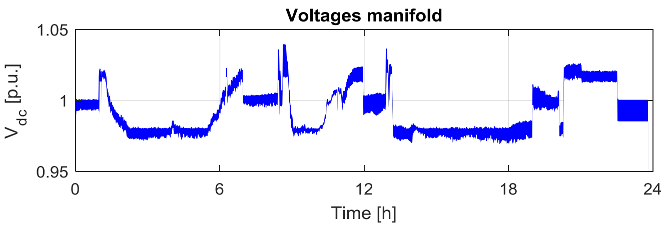

Fig. 8. Measured node voltages of the DC microgrid

It is worth noting that, even in presence of significant forecast errors, which would cause the drift of the batteries' SoC during operation, the developed control structure allows to adjust the state of charge of the batteries throughout the day and to keep the voltage close to the desired value. This test allows the verification of the ability.

5. CONCLUSIONS

This paper proposed and described the implementation of a hierarchical control scheme, for the integration of low-level controller, MPC and EMS of a DC microgrid. In the proposed approach, the energy management system provides the references for the model predictive controller by achieving an economical optimization. The MPC regulates the voltages in the network, as well as track the input signals received by the EMS control, and finally the low-level controller acts in a decentralized way via droop control. The applicability of the proposed scheme has been tested on the RSE's DC microgrid considering different control objectives and proving the validity of the given approach.

ACKNOWLEDGMENT

This work has been financed by the Research Fund for the Italian Electrical System in compliance with the Decree of Minister of Economical Development April 16, 2018

REFERENCES

Cucuzzella, M. et al., 2019. *Robust Passivity-Based Control of Boost Converters in DC Microgrids.* Nice, France, IEEE 58th Conference on Decision and Control (CDC).

Cucuzzella, M. et al., 2018. Sliding mode voltage control of boost converters in DC microgrids. *Control Engineering Practice,* Volume 73, pp. 161-170.

Cucuzzella, M., Trip, S. & Scherpen, J., 2018. A Consensus-Based Controller for DC Power Networks. *IFAC-PapersOnLine,* 51(33), pp. 205-210.

Dragičević, T., Lu, X., Vasquez, J. C. & Guerrero, J. M., 2016. DC Microgrids—Part I: A Review of Control Strategies and Stabilization Techniques. *IEEE Transactions on Power Electronics,* 31(7), pp. 4876-4891.

Dragicevic, T., Vasquez, J. C., Guerrero, J. M. & Skrlec, D., 2014. Advanced LVDC Electrical Power Architectures and Microgrids: A step toward a new generation of power distribution networks. *IEEE Electrification Magazine,* 2(1), pp. 54-65.

Eghtedarpour, N. & Farjah, E., 2012. Control strategy for distributed integration of photovoltaic and energy storage systems in DC micro-grids. *Renewable Energy,* Volume 45, pp. 96-110.

Grillo, S. et al., 2014. DC Islands in AC Smart Grids. *IEEE Transactions on Power Electronics,* 29(1), pp. 89-98.

Iovine, A., Rigaut, T., Damn, G. D. S. E. & Di Benedetto, M. D., 2019. Power management for a DC MicroGrid integrating renewables and storage. *Control Engineering Practice,* Volume 85, pp. 59-79.

L.Darby, M., Harmse, M. & Nikolaou, M., 2009. MPC: Current Practice and Challenges. *IFAC Proceedings Volumes,* 42(11), pp. 86-98.

Liang, C. & Mohammad, S., 2014. DC Microgrids: Economic Operation and Enhancement of Resilience by Hierarchical Control. *IEEE Transactions on Smart Grid,* 5(5), pp. 2517-2526.

Liu, G., Caldognetto, T. & Mattavelli, P., 2017. *Power-based droop control in DC microgrids enabling seamless disconnection from AC grids.* IEEE Second International Conference on DC Microgrids (ICDCM), Nuremburg, 2017, pp. 523-528., s.n.

Meng, L. et al., 2017. Review on Control of DC Microgrids and Multiple Microgrid Clusters. *IEEE Journal of Emerging and Selected Topics in Power Electronics,* 5(3), pp. 928-948.

Nasirian, V., Moayedi, S., Davoudi, A. & Lewis, F. L., 2015. Distributed Cooperative Control of DC Microgrids. *IEEE Transactions on Power Electronics,* 30(4), pp. 2288-2303.

Oliveira, T. R., Silva, W. W. A. G. & Donoso-Garcia, P. F., 2017. Distributed Secondary Level Control for Energy Storage Management in DC Microgrids. *IEEE Transactions on Smart Grid,* 8(6), pp. 2597 - 2607.

Papadimitriou, C. N., Zountouridou, E. I. & Hatziargyriou, N. D., 2015. Review of hierarchical control in DC microgrids. *Electric Power Systems Research,* Volume 122, pp. 159-167.

Pellegrino, L. & Lazzari, R., 2018. *Energetic and economical analysis for a LVDC residential district.* Bari, Italy, AEIT International Annual Conference.

Ronchegalli, D. & Lazzari, R., 2016. *Development of the control strategy for a direct current microgrid: A case study.* Capri, s.n.

Sandeep, A., Baylon, G. F. & Guerrero, J. M., 2013. Distributed Control to Ensure Proportional Load Sharing and Improve Voltage Regulation in Low-Voltage DC Microgrids. *IEEE Transactions on Power Electronics,* 28(4), pp. 1900 - 1913.